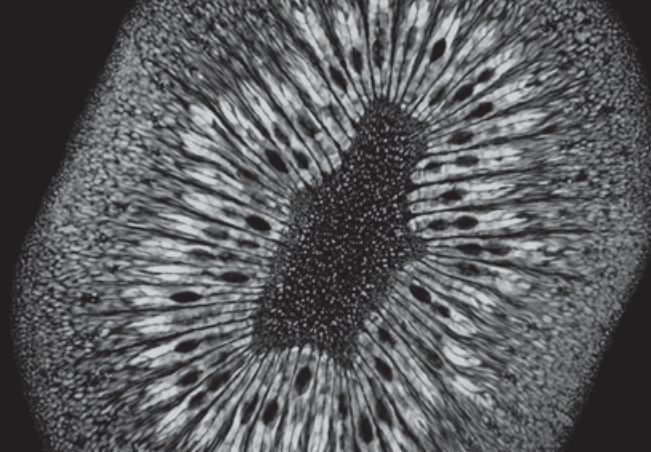
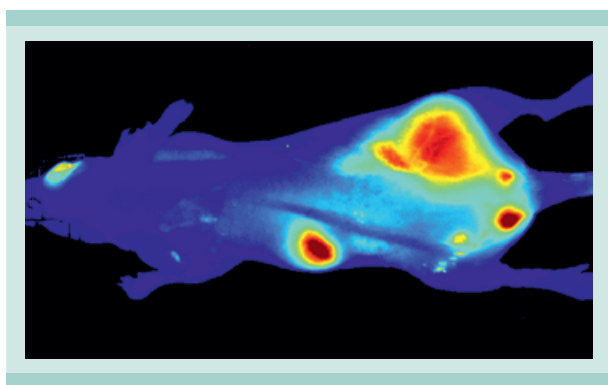


VISCOVER

Scintica:



Long-term tumor visualization



Long-term tumor visualization by NiraWave™ Rocker

Michael Hess¹, Jochen Stritzker^{2,1} and Aladar A. Szalay^{2,3,1}

¹ Department of Biochemistry, Biocenter, University of Würzburg, Würzburg, Germany

² Genelux Corporation, San Diego, CA, USA

³ Department of Radiation Oncology, Moores Cancer Center, University of California, San Diego, La Jolla, CA, USA

Introduction

Xenograft as well as homograft mouse models have become one of the most essential tools for cancer researchers in recent years. In particular, the search for new therapeutic agents has significantly amplified the importance of these models and has led to a widespread application of methods for monitoring the progression of tumor growth. Besides measurement via calipers, diagnostic imaging modalities are favored methods for tracking the tumor status *in vivo*. Especially optical imaging offers an easy, rapid and cost-effective avenue to take a closer look at tumors¹.

Despite the aforementioned advantages, optical imaging is still limited by the strong absorption of visible light by biological tissue as well as the strong autofluorescence of tissues below 600 nm. Therefore, near infrared dyes are privileged in terms of absorption and tissue penetration because of their excitation and emission in the so-called

optical window². In addition to these properties, an ideal agent for optical imaging of tumors would display a prolonged half-life in blood, to prevent rapid excretion, as well as a stable fluorescence, to allow longtime visualizations. In our research, which is mainly focused on the effect of a recombinant oncolytic vaccinia virus on different types of tumors³, we use virus-encoded reporter genes⁴ or stably transfected cell lines expressing fluorescent proteins to monitor tumor progression or metastases formation. Besides this, fundamental studies on the pharmacokinetics of prodrugs and the influence of the enhanced permeability and retention (EPR) effect⁵ led us to the use of the Viscover™ optical imaging agent, NiraWave™ Rocker.

Materials and methods

Human A549 lung adenocarcinoma (ATCC no. CCL-185), PC-3 prostate carcinoma (ATCC no. CRL-1435), as well as murine 4T1 mammary carcinoma (ATCC no. CRL-2539) cells were cultured under standard cell culture conditions. Implantation of tumor cells in the right hind flank of athymic nude or immunocompetent BALB/c mice was performed by injecting 2×10^6 (PC-3), 5×10^6 (A549) or 4×10^4 (4T1) cells, respectively. When tumors reached a size of approximately 300 mm³, 100 μ L NiraWave™ Rocker (Viscover™, nanoPET Pharma GmbH, Germany) were injected intravenously into the lateral tail vein of the mice. Fluorescent signals were monitored over several days to weeks using a Maestro™ Imaging System (CRI, Woburn, MA, USA) equipped with a NIR filter set (710–760 nm excitation filter and 800 nm long pass emission filter). Quantitative measurements were performed using the Maestro Software 2.10.0.

Results and discussion

Minutes after injection of NiraWave Rocker we observed a saturation effect, which led to a non-specific fluorescent signal over the whole mouse body. The highest fluorescence intensity was observed 20 minutes after injection signifying that excretion gains the upper hand at this point. After 9 hours, the majority of the dye seemed to be excreted and

a tumor-specific fluorescent signal was detectable indicating a retention effect of NiraWave Rocker in the tumor tissue. This effect could be observed in immunocompromised xenograft as well as in immunocompetent homograft models (Fig. 1A and Fig. 2A, upper row).

Although the tumor-specific fluorescent signal decreased over time, a specific detection of the carcinoma was possible even 14 days after injection of NiraWave Rocker (Fig. 1B). Even more significant is the fact that the tumor-to-body ratio increased over time reaching its maximum at day 14 with a factor of about 85 (Fig. 1C), allowing the distinction between

tumor- and body-tissue to become more precise over time. A comparison of tumor- and non-tumor-bearing mice confirmed the assumption that this effect is directly related to the presence of a tumor. No site-specific fluorescence could be observed in non-tumorous mice indicating that the EPR effect cannot be transferred to any other tissue in absence of a tumor (Fig. 2A and B).

Furthermore, a well-established model for lymph node metastases was used to examine whether the observed tumor-specific EPR effect can be related to metastasized lymph nodes. Indeed, 6 hours after injection of NiraWave Rocker

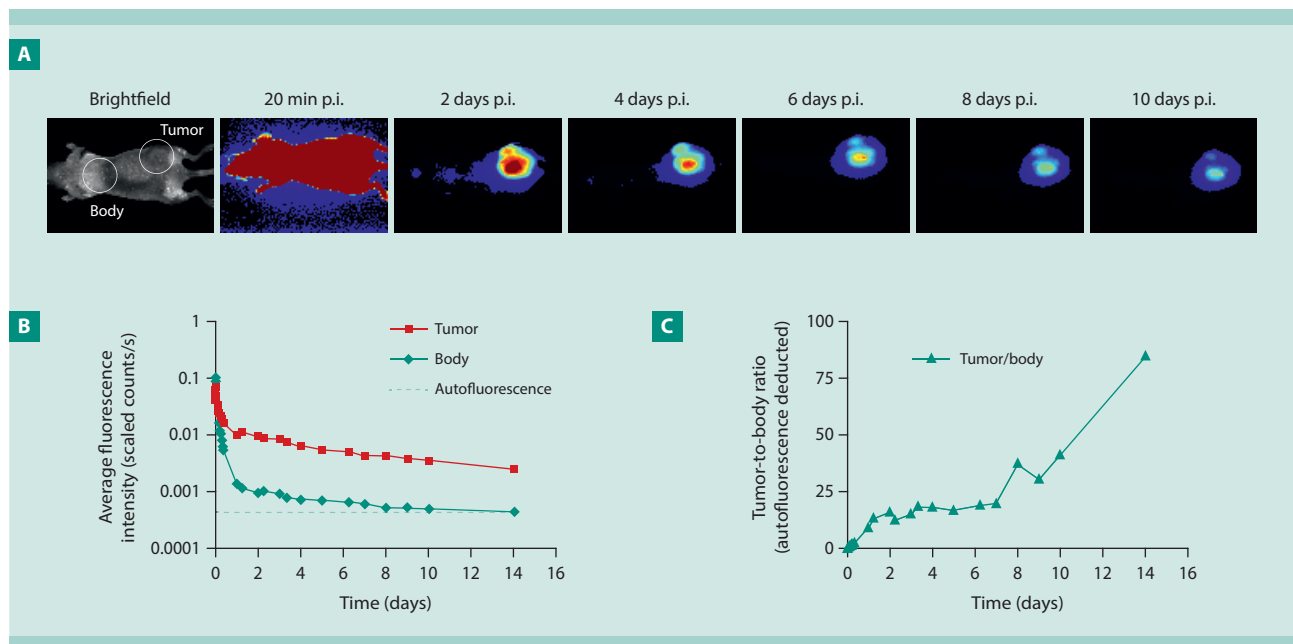


Figure 1: Time dependent fluorescence after systemic NiraWave Rocker injection in A549 tumor-bearing nude mice. **A.** Representative images of a mouse injected with NiraWave Rocker and monitored over 10 days. Intensities were scaled to maximum fluorescence (20 minutes post injection). **B.** Progress of body and tumor fluorescence intensity. **C.** Tumor-to-body ratio trend of detected fluorescent signals.

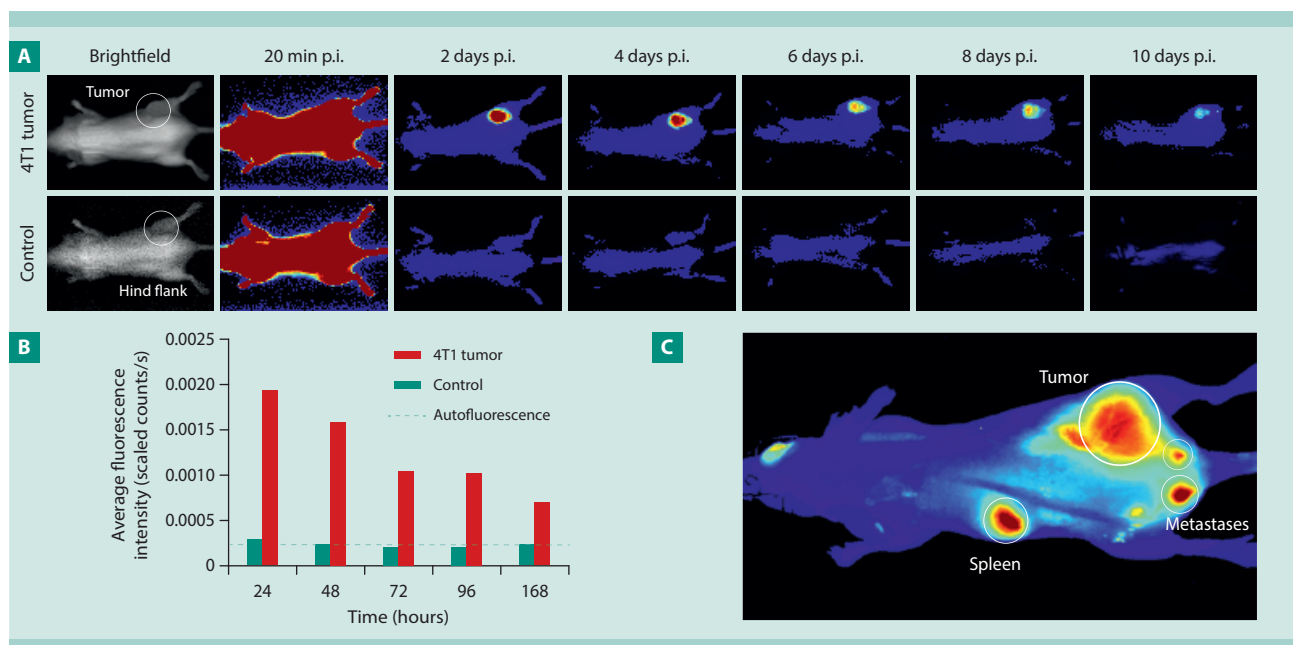


Figure 2: Biodistribution of NiraWave Rocker in immunocompetent hosts and in a metastatic tumor model. **A.** Time-dependent whole body fluorescence after NiraWave Rocker injection in tumorous and non-tumorous mice. **B.** Quantitative analysis of fluorescence intensities at the tumor region of the right hind flank of both tumor- and non-tumor-bearing mice. **C.** PC-3 tumor-bearing mouse with metastasized sciatic lymph nodes 6 hours after injection of NiraWave Rocker.

in a PC-3 tumor-bearing mouse with metastasized lymph nodes, far-red fluorescence could be detected in the spleen, tumor, and sciatic lymph node metastases (Fig. 2C). After 24 hours, these signals were still visible and led to the assumption that the EPR effect and its consequences can be visualized by NiraWave Rocker in tumorous as well as in metastatic animal models.

Conclusion

These first results signify that NiraWave Rocker presents cancer researchers with a great opportunity to study EPR effect phenomena, vasculature abnormalities, or the distribution pattern of, for example, chemotherapeutics based on nanomedicine in small animal xenograft as well as homograft models.

Acknowledgements

This research was supported by a Service Grant to the University of Würzburg, Germany, funded by Genelux Corp., San Diego, USA. The authors would like to thank Dr. Ulrike Donat for providing the PC-3 lymph node metastases-bearing animal model.

References

1. Graves, E.E. (2004) Fluorescence molecular imaging of small animal tumor models. *Curr. Mol. Med.* 4 (4): 419–430.
2. Tromberg, B.J. *et al.* (2000) Non-invasive *in vivo* characterization of breast tumors using photon migration spectroscopy. *Neoplasia*. 2: 26–40.
3. Zhang, Q. *et al.* (2007) Eradication of solid human breast tumors in nude mice with an intravenously injected light-emitting oncolytic vaccinia virus. *Cancer Res.* 67: 10038–10046.
4. Hess, M. *et al.* (2011) Bacterial glucuronidase as general marker for oncolytic virotherapy or other biological therapies. *J. Transl. Med.* 9: 172.
5. Matsumura, Y. and Maeda, H. (1986) A new concept for macromolecular therapeutics in cancer chemotherapy: mechanism of tumorotropic accumulation of proteins and the antitumor agent smancs. *Cancer Res.* 46: 6387–6392.

Viscover™ Product	Order No.
NiraWave™ C, 1 x 5 injections	130-095-154
NiraWave™ C, 5 x 5 injections	130-095-155
NiraWave™ M, 1 x 5 injections	130-095-156
NiraWave™ M, 5 x 5 injections	130-095-157
NiraWave™ Rocker, 1 x 5 injections	130-095-158
NiraWave™ Rocker, 5 x 5 injections	130-095-159
NiraWave™ nano 780, 1 x 5 injections	130-095-695
NiraWave™ nano 780, 5 x 5 injections	130-095-693

Scintica:

www.scintica.com

+1 (519) 914 5495
info@scintica.com

562 Waterloo St. London, ON,
Canada N6B 2P9